Excitons in a parabolic quantum dot in magnetic fields

V. Halonen
Department of Theoretical Physics, University of Oulu, Linnanmaa, SF-90570 Oulu 57, Finland

Tapash Chakraborty
Institute for Microstructural Sciences, National Research Council, Montreal Road, M-50, Ottawa, Canada K1A 0R6

P. Pietiläinen
Department of Theoretical Physics, University of Oulu, Linnanmaa, SF-90570 Oulu 57, Finland
(Received 30 August 1991; revised manuscript received 6 November 1991)

The properties of an exciton in a parabolic quantum dot in an external magnetic field are studied theoretically using an effective-mass Hamiltonian. The results for the energy and the optical absorption of the ground state and the low-lying excited states are presented. The Hamiltonian is written in terms of the center of mass and relative coordinates, and it is shown that, due to the coupling between the center of mass and relative motion, optical-absorption energies reveal an interesting anticrossing behavior. It is also shown that the ground-state properties are approximately determined by that part of the total Hamiltonian that depends only on the relative coordinates.

I. INTRODUCTION

A system of electrons and holes moving in two dimensions with their transverse motion quantized in the lowest level and subjected to a strong perpendicular magnetic field is known to exhibit many interesting properties.[1–5] It should be mentioned that in the single-component case of electrons (or holes) in a similar situation with the lowest Landau level partially filled, a remarkable many-electron phenomenon known as the fractional quantum Hall effect was discovered some years ago.[6] It is therefore quite natural to investigate what a two-component (electron and hole) system has in store. In the *ideal* two-dimensional case where the electron and hole wave functions are considered to be identical, Lerner and Lozovik[1] (and later, Rice, Paquet, and Ueda[2]) found that the *exact* ground state is a Bose condensate of noninteracting magnetic excitons. Another interesting result found by Rice, Paquet, and Ueda was that there is no plasma oscillation in this system—a consequence of the confinement to the lowest Landau level. The collective excitation is simply given by the *single-exciton* dispersion relation which is a result of the ideal Bose character of the ground state.

In this paper, we have added another dimension to our present understanding of the excitons in a magnetic field discussed above by placing an exciton in a zero-dimensional *parabolic quantum dot* structure.[7] These systems are of much current interest in order to develop an understanding of the mesoscopic physics in reduced dimensionality. Recent experimental work on quantum dots in a magnetic field[8] has demonstrated the interplay between the competing spatial and magnetic quantization and other subtle features due to electron correlations. Theoretical studies[9,10] have revealed the interesting role of electron correlations in these quantum confined systems. Earlier work by Bryant on excitons[11] and biexcitons[12] in quantum boxes (in the absence of a magnetic field) demonstrated the competing effects of quantum confinement and Coulomb-induced electron-hole correlations. Excitons and biexcitons have also been studied recently in semiconductor microcrystallites by Koch *et al.*[13–15] It should be pointed out that the measurement of the exciton binding energy in the presence of a magnetic field has been reported in quantum wells[16] and quantum wires.[17]

In Sec. II, we briefly describe the formalism and numerical techniques used to calculate the ground-state properties of an exciton in a quantum dot subjected to an external magnetic field. For simplicity, we have considered only the parabolic confinement of the electrons and holes. In some of the calculations, we also left the hole unconfined in the two-dimensional plane. Some of the computational steps are discussed briefly in this section. The results for the ground-state and low-lying excitation energies, electron-hole separation, and normalized intensity of the optical absorption are presented and discussed in Sec. III. A brief discussion and conclusion are given in Sec. IV.

II. THEORY

Our model Hamiltonian for a two-dimensional hydrogenic exciton in a parabolic confinement potential and in a static external magnetic field is

$$\mathcal{H}=\mathcal{H}_e+\mathcal{H}_h+\mathcal{H}_{e\text{-}h} , \tag{1}$$

where the electron, hole, and electron-hole terms are

$$\mathcal{H}_e=\frac{1}{2m_e}\left[-i\hbar\nabla_e-\frac{e}{c}\mathbf{A}_e\right]^2+\tfrac{1}{2}m_e\omega_e^2 r_e^2 ,$$
$$\mathcal{H}_h=\frac{1}{2m_h}\left[-i\hbar\nabla_h+\frac{e}{c}\mathbf{A}_h\right]^2+\tfrac{1}{2}m_h\omega_h^2 r_h^2 , \tag{2}$$
$$\mathcal{H}_{e\text{-}h}=-\frac{e^2}{\epsilon}\frac{1}{|\mathbf{r}_e-\mathbf{r}_h|} .$$

Here ϵ is the background dielectric constant. We calculate the eigenfunctions and eigenvalues of the system using the method of numerical diagonalization of the Hamiltonian. In this method the Hamiltonian of the system is divided into two parts, $\mathcal{H}=\mathcal{H}_0+\mathcal{H}'$, where $\mathcal{H}_0$ is the Hamiltonian for the noninteracting system. The term $\mathcal{H}'$ then includes all the interactions between the particles. The eigenfunctions of $\mathcal{H}$ are expanded in terms of the eigenfunctions of $\mathcal{H}_0$. The original problem of finding eigenfunctions and eigenvalues of $\mathcal{H}$ is now transformed to a problem of diagonalizing a matrix whose components are $\langle\varphi_i|\mathcal{H}|\varphi_j\rangle$, where the φ_i's are the eigenfunctions of $\mathcal{H}_0$. In the actual numerical calculations the number of basis functions φ_i must be finite. Usually the basis functions are chosen such that they are the lowest-energy states of the Hamiltonian $\mathcal{H}_0$.

One possible approach within the diagonalization scheme is to expand the wave functions of the system in terms of the eigenfunctions of the noninteracting electron-hole pair, i.e., we select $\mathcal{H}_0=\mathcal{H}_e+\mathcal{H}_h$ and $\mathcal{H}'=\mathcal{H}_{e\text{-}h}$. The eigenfunctions of $\mathcal{H}_e$ and $\mathcal{H}_h$ are

$$\Psi_{n_\alpha l_\alpha}=\left[\frac{a_\alpha}{\pi}\frac{n_\alpha!}{(n_\alpha+|l_\alpha|)!}\right]^{1/2}\times\exp[-il_\alpha\Theta_\alpha-(a_\alpha r_\alpha)^2/2]\times(a_\alpha r_\alpha)^{l_\alpha}L_{n_\alpha}^{|l_\alpha|}[(a_\alpha r_\alpha)^2]\ , \tag{3}$$

where α denotes the electron or hole, $a_\alpha=[(\omega_\alpha^2+\omega_c^2/4)^{1/2}m_\alpha/\hbar]^{1/2}$, $L_n^{|l|}$ are the associated Laguerre polynomials, ω_c is the cyclotron frequency, and l and n are the angular and radial quantum numbers, respectively. The advantage of this method is that the interaction matrix elements between the noninteracting electron-hole pair states can be expressed in a closed form:

$$\begin{aligned}
&\langle n_e^i l_e^i n_h^i l_h^i|\mathcal{H}_{e\text{-}h}|n_e^j l_e^j n_h^j l_h^j\rangle \\
&=-\frac{e^2}{\epsilon}a_e\delta_{l_e^i+l_h^i,l_e^j+l_h^j}\left[\frac{n_e^i!}{(|l_e^i|+n_e^i)!}\frac{n_h^i!}{(|l_h^i|+n_h^i)!}\frac{n_e^j!}{(|l_e^j|+n_e^j)!}\frac{n_h^j!}{(|l_h^j|+n_h^j)!}\right]^{1/2} \\
&\times\sum_{\alpha=0}^{n_e^i}\sum_{\beta=0}^{n_e^j}\sum_{\gamma=0}^{n_h^i}\sum_{\delta=0}^{n_h^j}[\alpha+\beta+\tfrac{1}{2}(|l_e^i|+|l_e^j|-k)]![\gamma+\delta+\tfrac{1}{2}(|l_h^i|+|l_h^j|-k)]! \\
&\times\frac{(-1)^{\alpha+\beta}}{\alpha!\beta!}\frac{(|l_e^i|+n_e^i)!(|l_e^j|+n_e^j)!}{(|l_e^i|+\alpha)!(n_e^i-\alpha)!(|l_e^j|+\beta)!(n_e^j-\beta)!} \\
&\times\frac{(-1)^{\gamma+\delta}}{\gamma!\delta!}\frac{(|l_h^i|+n_h^i)!(|l_h^j|+n_h^j)!}{(|l_h^i|+\gamma)!(n_h^i-\gamma)!(|l_h^j|+\delta)!(n_h^j-\delta)!} \\
&\times\sum_{p=0}^{\alpha+\beta+1/2(|l_e^i|+|l_e^j|-k)}\frac{[\alpha+\beta+\frac{1}{2}(|l_e^i|+|l_e^j|+k)]!}{[\alpha+\beta+\frac{1}{2}(|l_e^i|+|l_e^j|-k)-p]!(k+p)!} \\
&\times\sum_{s=0}^{\gamma+\delta+1/2(|l_h^i|+|l_h^j|-k)}\frac{[\gamma+\delta+\frac{1}{2}(|l_h^i|+|l_h^j|+k)]!}{[\gamma+\delta+\frac{1}{2}(|l_h^i|+|l_h^j|-k)-s]!(k+s)!} \\
&\times\frac{(-1)^{p+s}}{p!s!}\frac{(a_e/a_h)^{2s+k}\Gamma(k+p+s+\frac{1}{2})}{[1+(a_e/a_h)^2]^{k+p+s+1/2}}\ ,
\end{aligned} \tag{4}$$

where $k=|l_e^i-l_e^j|$. Unfortunately this approach leads to a poor convergence of the eigenvalues as a function of the number of basis states. A better way is to introduce the center of mass (c.m.) and relative coordinates $\mathbf{R}=(1/M)(m_e\mathbf{r}_e+m_h\mathbf{r}_h)$, $\mathbf{r}=\mathbf{r}_e-\mathbf{r}_h$, where we have adopted the usual notations: $M=m_e+m_h$, $\mu=m_e m_h/M$, and $\gamma=(m_h-m_e)/M$. We also choose the symmetric gauge vector potentials for the electrons and holes as $\mathbf{A}_e=\frac{1}{2}\mathbf{B}\times(\mathbf{r}_e-\mathbf{r}_h)$ and $\mathbf{A}_h=-\frac{1}{2}\mathbf{B}\times(\mathbf{r}_e-\mathbf{r}_h)$. The Hamiltonian (1) can then be written in the form

$$\mathcal{H}=\mathcal{H}_{\text{c.m.}}+\mathcal{H}_{\text{rel}}+\mathcal{H}_x\ , \tag{5}$$

where the c.m., relative, and the cross term of the Hamiltonian are

$$\begin{aligned}
\mathcal{H}_{\text{c.m.}}&=-\frac{\hbar^2}{2M}\nabla_{\text{c.m.}}^2+\tfrac{1}{2}M\left[\frac{1}{M}(m_e\omega_e^2+m_h\omega_h^2)\right]R^2\ , \\
\mathcal{H}_{\text{rel}}&=-\frac{\hbar^2}{2\mu}\nabla_{\text{rel}}^2+\frac{i\hbar e}{2\mu c}\gamma\mathbf{B}\cdot\mathbf{r}\times\nabla_{\text{rel}} \\
&\quad+\tfrac{1}{2}\mu\left[\frac{e^2B^2}{4\mu^2c^2}+\frac{1}{M}(m_h\omega_e^2+m_e\omega_h^2)\right]r^2-\frac{e^2}{\epsilon}\frac{1}{r}\ , \\
\mathcal{H}_x&=\frac{i\hbar e}{Mc}\mathbf{B}\cdot\mathbf{r}\times\nabla_{\text{c.m.}}+\mu(\omega_e^2-\omega_h^2)\mathbf{R}\cdot\mathbf{r}\ .
\end{aligned} \tag{6}$$

In Eq. (6), $\mathcal{H}_{\text{c.m.}}$, which depends only on the c.m. coordinate, is the Hamiltonian of a well-known two-dimensional harmonic oscillator with energy spectrum

$$E_{\text{c.m.}}=(2n_{\text{c.m.}}+|l_{\text{c.m.}}|+1)\hbar\omega_{\text{c.m.}} \tag{7}$$

and

$$\omega_{\text{c.m.}}=\left[\frac{1}{M}(m_e\omega_e^2+m_h\omega_h^2)\right]^{1/2}, \tag{8}$$

with $n_{\text{c.m.}}\geq 0$. Also, $\mathcal{H}_{\text{rel}}$ is a Hamiltonian of a two-dimensional charged particle in a magnetic field and in parabolic and Coulomb potentials. It can be further separated into radial and angular parts. The radial part of the Schrödinger equation

$$R''+\frac{1}{r}R'+\left[\frac{2\mu}{\hbar^2}\left[E+\frac{e^2}{\epsilon}\frac{1}{r}\right]-\frac{l_{\text{rel}}^2}{r^2}-\left[\frac{e^2B^2}{4\hbar^2c^2}+\frac{\mu^2}{M\hbar^2}(m_h\omega_e^2+m_e\omega_h^2)\right]r^2\right]R=0 \tag{9}$$

can be solved numerically using a standard method called *shooting to a fitting point.*[18] Briefly, the method is to guess the value of E and to integrate the differential equation from zero to some point r_f (called the fitting point) and from infinity (i.e., from a point which is far enough from the origin) to the same point r_f. For the correct E we require that both the solution R and its first derivative are continuous at the fitting point r_f. The eigenfunctions are labeled by the angular momentum l_{rel} and by the principal quantum number n_{rel}. The contribution of the relative motion Hamiltonian $\mathcal{H}_{\text{rel}}$ to the total energy is

$$E_{\text{rel}}=E-\gamma\frac{eB}{2\mu c}l_{\text{rel}}\ . \tag{10}$$

Finally, all interactions between c.m. and relative motions are included in the cross term $\mathcal{H}_x$. Eigenfunctions and eigenvalues of the system can now be calculated accurately using the eigenfunctions of $\mathcal{H}_{\text{c.m.}}+\mathcal{H}_{\text{rel}}$ as basis functions for the numerical diagonalization of the total Hamiltonian $\mathcal{H}$. Because the contribution of interaction $\mathcal{H}_x$ was found to be relatively small only a small number of basis states was needed in the actual calculations. One final note about $\mathcal{H}_{\text{rel}}$: here the harmonic term is $\frac{1}{2}[\omega_c^2+(1/M)(m_h\omega_e^2+m_e\omega_h^2)]r^2$, where $(1/M)(m_h\omega_e^2+m_e\omega_h^2)$ is *different* from $\omega_{\text{c.m.}}^2=(1/M)(m_e\omega_e^2+m_h\omega_h^2)$. One cannot therefore simply replace ω_c in the two-dimensional calculations of Ref. 5 by $(\omega_c^2+\omega_{\text{c.m.}}^2)^{1/2}$ to obtain our results described below.

In addition to the ground-state and low-lying excitation energies we also present the numerical results for the electron-hole separation and the intensity of the optical absorption. The electron-hole separation can be calculated as an expectation value of the relative coordinate:

$$\langle r\rangle=\sum_{i,j}c_i^*c_j\langle n_{\text{rel}}^i l_{\text{rel}}^i|r|n_{\text{rel}}^j l_{\text{rel}}^j\rangle \times\delta_{n_{\text{c.m.}}^i,n_{\text{c.m.}}^j}\delta_{l_{\text{c.m.}}^i,l_{\text{c.m.}}^j},$$

where the c_i's are the expansion coefficient of the ground state. Because the eigenfunctions $|n_{\text{rel}}^i l_{\text{rel}}^i\rangle$ of the Hamiltonian $\mathcal{H}_{\text{rel}}$ can be obtained only numerically, the matrix elements $\langle n_{\text{rel}}^i l_{\text{rel}}^i|r|n_{\text{rel}}^j l_{\text{rel}}^j\rangle$ are calculated using numerical integration. In order to compare with the results obtained in Ref. 12 for a confined exciton (in the absence of a magnetic field) we have also calculated the quantity $(\langle r^2\rangle)^{1/2}$. The normalized intensity of optical absorption is calculated as an expectation value,

$$\langle\delta(\mathbf{r})\rangle=\sum_{i,j}c_i^*c_jR_{n_{\text{rel}}^i l_{\text{rel}}^i}(0)R_{n_{\text{rel}}^j l_{\text{rel}}^j}(0) \times\delta_{l_{\text{rel}}^i,l_{\text{rel}}^j}\delta_{n_{\text{c.m.}}^i,n_{\text{c.m.}}^j}\delta_{l_{\text{c.m.}}^i,l_{\text{c.m.}}^j},$$

which gives the probability of finding the electron and hole at the same position.

III. RESULTS

In this section we present the numerical results for the parameters appropriate to GaAs, i.e., dielectric constant $\epsilon=13.1$, electron effective mass $m_e=0.067m$, and hole effective mass $m_h=0.090m$ for light holes and $m_h=0.377m$ for heavy holes.[12] We should point out that by a *light (heavy) hole* we mean a hole that has light (heavy) in-plane mass. In Ref. 12, the opposite convention was employed. Let us first compare the results of the two approaches described in the preceding section. The ground-state energy of a heavy-hole exciton as a function of confinement potential energy ($\omega_e=\omega_h$) in the absence of the magnetic field is shown in Fig. 1. As the interaction between c.m. and relative motions $\mathcal{H}_x$ in this case is equal to zero, the c.m. and relative motion separation approach is exact within the numerical accuracy of the shooting method that was used to calculate the eigenvalues of $\mathcal{H}_{\text{rel}}$. It is seen from Fig. 1 that at low confinement energies when the electron-hole pair is strongly correlated due to the Coulomb force, the noninteracting electron-hole pair state basis approach needs a very large number of basis states to converge. When the confinement energy is increased the noninteracting

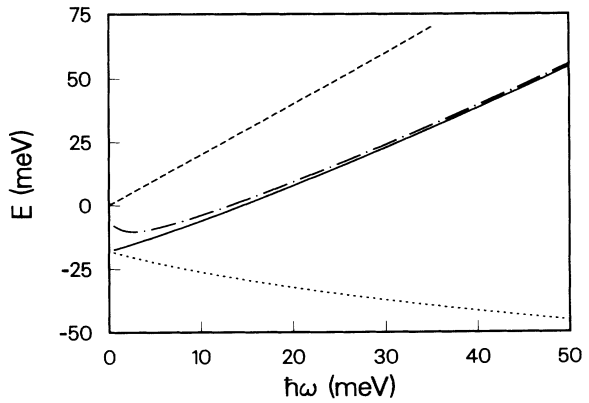

FIG. 1. The ground-state energy of a heavy-hole ($m_h=0.377m$) exciton as a function of a single-particle confinement potential energy ($\hbar\omega_e=\hbar\omega_h$). The solid curve is calculated using c.m. and relative motion separation and the dot-dashed curve is calculated using the noninteracting electron-hole pair state basis (500 basis states). The energy of a noninteracting electron-hole pair (dashed curve) and the Coulomb-interaction energy (dotted curve) are also shown.

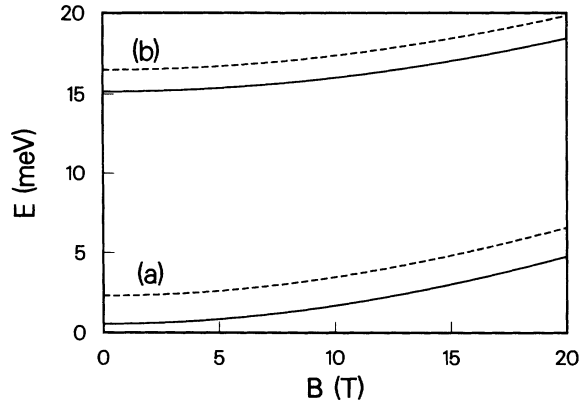

FIG. 2. The ground-state energy of a heavy-hole ($m_h=0.377m$) exciton as a function of the magnetic field B (T). Confinement potential energy for both electron and hole is (a) 15.0 meV and (b) 25.0 meV. Solid curves are calculated using c.m. and relative motion separation and dashed curves are calculated using the noninteracting electron-hole pair state basis (500 basis states) as explained in the text.

electron-hole pair states give a better description of the system, although the magnitude of the Coulomb interaction $\mathcal{H}_{e\text{-}h}$ is also increased. Another comparison between our numerical approaches is given in Fig. 2, where we have plotted the ground-state energy of a heavy-hole exciton as a function of the external magnetic field. It is quite apparent that both approaches give the same magnetic-field dependence. This indicates that the correlations do not change as a function of the magnetic field.

In the numerical results presented in Figs. 1 and 2 we have used the same confinement potential energy for both electron and hole. One other possibility is to leave the hole unconfined within the two-dimensional plane. In that case the hole is moving freely in the plane and it feels only the electrostatic potential of the electron and the external magnetic field. In Fig. 3 we have plotted the ground-state energies of heavy- and light-hole excitons as a function of the confinement potential energy of the electron when the hole is not confined within the plane. Comparing Figs. 1 and 3 it is evident that the ground-state energy as a function of the confinement energy is not increasing as rapidly as in the case of equal confinement potential energy for both particles. The main contribution for this comes from the behavior of $\mathcal{H}_{\text{c.m.}}$ and $\mathcal{H}_{\text{rel}}$. In Fig. 3 we have also plotted the ground-state energy calculated without the cross term $\mathcal{H}_x$. Interaction between c.m. and relative motions is attractive for both light- and heavy-hole excitons, thereby lowering the ground-state energy.

We have calculated the ground-state energy, the electron-hole separation, and the relative intensity of the optical absorption as a function of the magnetic field with various confinement potential energies (Figs. 4–6). In all these calculations we have left the hole unconfined within the plane. In Fig. 4 the ground-state energies with and without the cross term between c.m. and relative motions are shown. As a comparison, the result for a purely two-dimensional exciton is also shown. For a two-dimensional exciton ($\hbar\omega_e=\hbar\omega_h=0$) our numerical calculations reproduce the results of Shinada and Tanaka.[5] The effect of the cross term $\mathcal{H}_x$ to the ground-state energy is relatively small. Therefore, as a first approximation, we can explain the ground-state properties of the exciton using the Hamiltonian $\mathcal{H}_{\text{c.m.}}+\mathcal{H}_{\text{rel}}$. At low confinement potential energies the ground-state energy is increasing approximately quadratically as a function of the magnetic field. This is due to the B^2 coefficient in the harmonic term in $\mathcal{H}_{\text{rel}}$. But because the harmonic term is proportional to the sum of the squares of the magnetic field and of the confinement potential energy, the effect of the magnetic field is decreased when the confinement potential energy is increased. Another interesting feature seen from Fig. 4 is that the effect of the cross term $\mathcal{H}_x$ to the ground-state energy is nearly independent of the magnet-

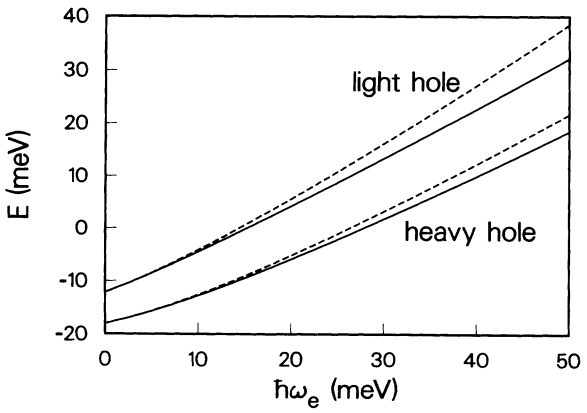

FIG. 3. The ground-state energy of a heavy-hole ($m_h=0.377m$) and a light-hole ($m_h=0.09m$) exciton as a function of confinement potential energy of the electron with (solid curve) and without (dashed curve) the cross term between c.m. and relative motion. The hole is unconfined in the two-dimensional plane.

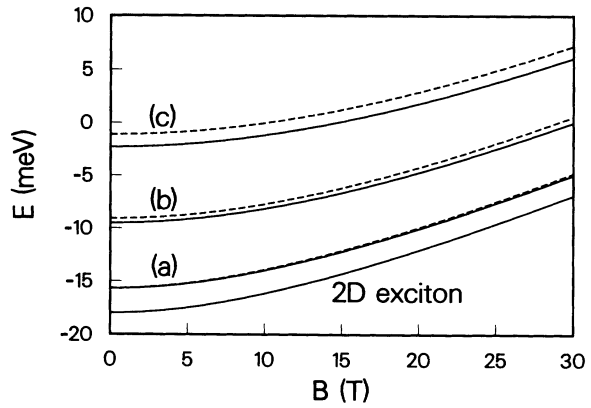

FIG. 4. The ground-state energy of a heavy-hole ($m_h=0.377m$) exciton as a function of the magnetic field (T). Confinement potential energy for the electron is (a) $\hbar\omega_e=5.0$ meV, (b) $\hbar\omega_e=15.0$ meV, and (c) $\hbar\omega_e=25.0$ meV. The hole is unconfined within the two-dimensional plane. The lowest curve is the result for a two-dimensional exciton. Energies without the cross term between c.m. and relative motion are also plotted (dashed curves).

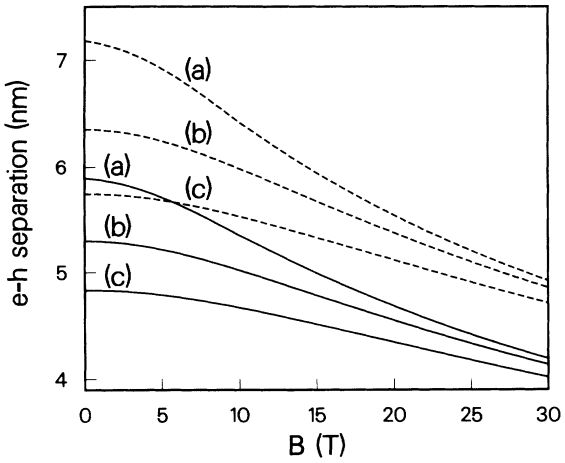

FIG. 5. The ground-state electron-hole separation of a heavy-hole ($m_h=0.377m$) exciton as a function of the magnetic field (T). Confinement potential energy for the electron is (a) $\hbar\omega_e=5.0$ meV, (b) $\hbar\omega_e=15.0$ meV, and (c) $\hbar\omega_e=25.0$ meV. The hole is unconfined within the two-dimensional plane. Electron-hole separation is calculated as $\langle r\rangle$ (solid curves). We have also plotted $(\langle r^2\rangle)^{1/2}$ (dashed curves).

ic field.

In Fig. 5 the numerical results for the ground-state electron-hole separation of an exciton as a function of the magnetic field are shown. The separation is, as expected, largest at low confinement and at low magnetic fields and approaches zero when the confinement potential energy and magnetic field are increased significantly. The decrease of the magnetic-field dependence is biggest near 10 T. The influence of the external magnetic field on the electron-hole separation is surprisingly small. For example, when the confinement potential energy for the electron is 5 meV the size of the exciton is reduced only by about 30% as the magnetic field is increased from 0 to 30 T. For higher values of the confinement energy the effect of the magnetic field is even smaller.

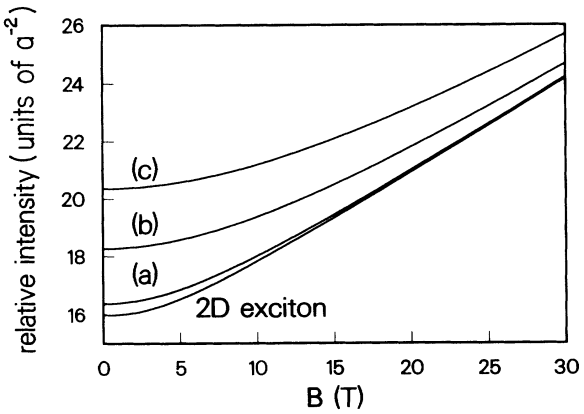

FIG. 6. Normalized intensity of the optical absorption calculated for the ground state of a heavy-hole ($m_h=0.377m$) exciton as a function of the magnetic field (T). Confinement potential energy for the electron is (a) $\hbar\omega_e=5.0$ meV, (b) $\hbar\omega_e=15.0$ meV, and (c) $\hbar\omega_e=25.0$ meV. The hole is unconfined within the two-dimensional plane. The lowest curve is the result for a two-dimensional exciton. The normalized intensity is measured in units of a^{-2}, where $a=\epsilon\hbar^2/\mu e^2$ is the effective Bohr radius.

The behavior of the ground-state optical-absorption intensity as a function of the magnetic field and confinement potential energy is presented in Fig. 6. The results are in line with the results of the ground-state energy and the electron-hole separation calculations. The increase of confinement suppresses the effect of the magnetic field and vice versa. The intensity of optical absorption increases with increasing magnetic field.

In Fig. 7 we have presented the results for the lowest energy levels of a light-hole ($m_h=0.09m$) exciton as a function of the magnetic field without (a) and with (b) the cross term $\mathcal{H}_x$ in the Hamiltonian. We have plotted only those levels that have the total angular momentum $L=0$. Although the effect of the cross term $\mathcal{H}_x$ is much larger for the excited states than for the ground state, we can identify at least some of the lowest levels using the noninteracting energy levels [Fig. 7(a)]. Because of the confinement, the relative angular momentum of the exciton can have different angular momentum values to give the total angular momentum $L=0$. In Fig. 7(a) the energy levels for the relative angular momentum $l_{\rm rel}=0$ (solid curves) and $l_{\rm rel}=\pm1$ (dashed curves) are shown. For each energy level of the relative motion there is a spectrum of the c.m. levels separated from each other by the amount of the confinement potential energy. To illustrate this feature more clearly we have labeled each level by its (exact) quantum numbers: $n_{\rm c.m.}$, $l_{\rm c.m.}$, $n_{\rm rel}$, and $l_{\rm rel}$. When the cross term $\mathcal{H}_x$ is included in the Hamiltonian, many anticrossings are revealed in the energy spectrum [Fig. 7(b)]. In addition to these anticrossings, it can be

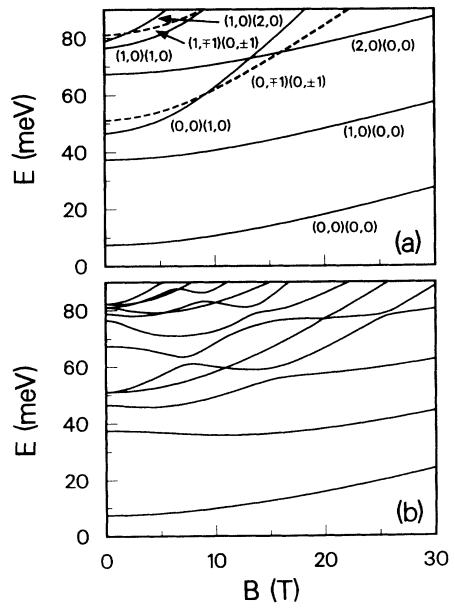

FIG. 7. The ground-state and low-lying excitation energies of a light-hole ($m_h=0.09m$) exciton as a function of the magnetic field (T) without (a) and with (b) the cross term between c.m. and relative motion. The angular momentum is $l_{\rm c.m.}+l_{\rm rel}=0$. Confinement potential energy is 15 meV for both particles. In (a) the energy levels are labeled by their quantum numbers, which are shown in parentheses as $(n_{\rm c.m.},l_{\rm c.m.})(n_{\rm rel},l_{\rm rel})$.

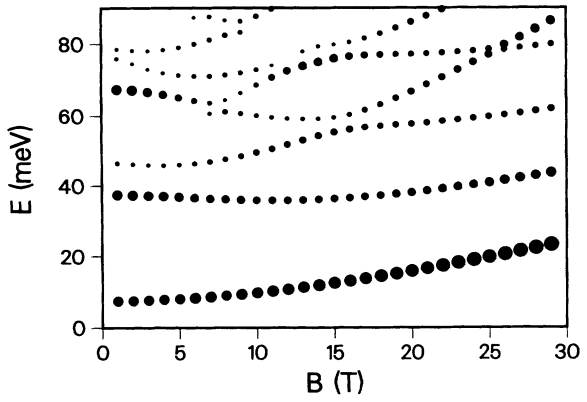

FIG. 8. Optical-absorption energies and intensities of a light-hole ($m_h=0.09m$) exciton as a function of the magnetic field (T). Confinement potential energy is 15 meV for both particles. Diameters of the filled points are proportional to the calculated intensity of the absorption.

seen that when the magnetic field is increased some of the energy levels begin to form the first and second Landau levels.

We have also calculated the intensity of the optical absorption for all of the energy levels shown in Fig. 7(b). The results of these calculations are plotted in Fig. 8, where a rich anticrossing structure of the optically active energy levels is still present. Because we have used an effective-mass approximation, the effects of the valence-band mixing have not been taken into account in our calculations. In reality the energy levels of light- and heavy-hole excitons are coupled leading to an even more complicated structure of the magneto-optical energy spectrum than we have in our calculations. Nevertheless, our results predict that it should be possible to evaluate from magneto-optical measurements the binding energy of the exciton and the strength of the confinement potential.

IV. DISCUSSION AND CONCLUSIONS

We have presented results for a single exciton in a parabolic quantum dot in the presence of a magnetic field. We have discused in detail different numerical approaches employed in obtaining the results. The numerical results for the ground-state and low-lying excitation energies are presented. We have also presented the results for the electron-hole separation and the intensity for optical absorption for an exciton where the electron is confined in a parabolic potential and the hole is left unconfined within the two-dimensional plane. Magneto-optical measurements in quasi-zero-dimensional exciton systems have just begun.[19] It is expected that the theoretical results presented here might provide useful insights on the experimental investigations of excitons in a quantum dot in magnetic fields.

ACKNOWLEDGMENTS

One of us (T.C.) would like to thank Dr. K. Kash (Bellcore) for several helpful discussions.

[1]I. V. Lerner and Yu. E. Lozovik, Zh. Eksp. Teor. Fiz. **80**, 1448 (1981) [Sov. Phys. JETP **53**, 763 (1981)].

[2]T. M. Rice, D. Paquet, and K. Ueda, Phys. Rev. B **32**, 5208 (1985); Helv. Phys. Acta **58**, 410 (1985).

[3]C. Kallin and B. I. Halperin, Phys. Rev. B **30**, 5655 (1984).

[4]L. P. Gorkov and I. E. Dzyaloshinskii, Zh. Eksp. Teor. Fiz. **53**, 717 (1967) [Sov. Phys. JETP **26**, 449 (1968)].

[5]M. Shinada and S. Sugano, J. Phys. Soc. Jpn. **21**, 1936 (1966); O. Akimoto and H. Hasegawa, *ibid.* **22**, 181 (1967); M. Shinada and K. Tanaka, *ibid.* **29**, 1258 (1970).

[6]D. C. Tsui, H. L. Störmer, and A. C. Gossard, Phys. Rev. Lett. **48**, 1559 (1982); Tapash Chakraborty and P. Pietiläinen, *The Fractional Quantum Hall Effect* (Springer-Verlag, New York, 1988).

[7]A preliminary report on these calculations was given by Tapash Chakraborty and V. Halonen, in *Proceedings of the International Symposium on Nanostructures and Mesoscopic Systems, Santa Fe, New Mexico* (Academic, New York, in press).

[8]T. Demel, D. Heitmann, P. Grambow, and K. Ploog, Phys. Rev. Lett. **64**, 788 (1990); W. Hansen, T. P. Smith III, K. Y. Lee, J. M. Hong, and C. M. Knoedler, Appl. Phys. Lett. **56**, 168 (1990); Ch. Sikorski and U. Merkt, Phys. Rev. Lett. **62**, 2164 (1989).

[9]P. A. Maksym and Tapash Chakraborty, Phys. Rev. Lett. **65**, 108 (1990); Tapash Chakraborty, V. Halonen, and P. Pietiläinen, Phys. Rev. B **43**, 14 289 (1991).

[10]G. W. Bryant, Phys. Rev. Lett. **59**, 1140 (1987).

[11]G. W. Bryant, Phys. Rev. B **37**, 8763 (1988); Surf. Sci. **196**, 596 (1988).

[12]G. W. Bryant, Phys. Rev. B **41**, 1243 (1990).

[13]Y. Z. Hu, M. Lindberg, and S. W. Koch, Phys. Rev. B **42**, 1713 (1990).

[14]Y. Z. Hu, S. W. Koch, M. Lindberg, N. Peyghambarian, E. L. Pollock, and F. A. Abraham, Phys. Rev. Lett. **64**, 1805 (1990).

[15]E. L. Pollock and S. W. Koch, J. Chem. Phys. **94**, 6776 (1991); E. L. Pollock and K. J. Runge (unpublished).

[16]J. C. Maan, G. Belle, A. Fasolino, M. Altarelli, and K. Ploog, Phys. Rev. B **30**, 2253 (1984); D. C. Rogers, J. Singleton, R. J. Nicholas, C. T. Foxon, and K. Woodbridge, *ibid.* **34**, 4002 (1986); W. Ossau, B. Jäkel, E. Bangert, G. Landwehr, and G. Weimann, Surf. Sci. **174**, 188 (1986).

[17]M. Kohl, D. Heitmann, P. Grambow, and K. Ploog, Phys. Rev. Lett. **63**, 2124 (1989).

[18]W. H. Press, B. P. Flannery, S. A. Teukolsky, and W. T. Vetterling, *Numerical Recipes in C: The Art of Scientific Computing* (Cambridge University Press, Cambridge, 1988), p. 606.

[19]K. Kash, J. Lumin. **46**, 69 (1990).